Conformational Diversity of the Fibrillogenic Fusion Peptide B18 in Different Environments from Molecular Dynamics Simulations

Volker Knecht,* Helmut Möhwald, and Reinhard Lipowsky

Max Planck Institute of Colloids and Interfaces, Science Park Golm, 14424 Potsdam, Germany

Received: September 11, 2006; In Final Form: January 12, 2007

The development of specific agents against amyloidoses requires an understanding of the conformational behavior of fibrillogenic peptides in different environments on the microscopic level. We present extensive molecular dynamics simulations of the fibrillogenic Bindin (103−120) B18 fusion peptide for several different environments: a water−trifluorethanol (TFE) mixture, pure water, aqueous buffer containing 100 mM NaCl, and a buffer−vapor interface. The peptide was studied as an isolated molecule in solution or at an interface. In the simulations, the conformational behavior of the peptide was found to strongly depend on the environment in agreement with experimental data. Overall, large portions of the peptide were unstructured. Preformed α-helical conformations were least stable in pure water and most stable in the water−TFE mixture and the buffer−vapor interface. In all environments, the α-helical conformation was most stable in the region around residues 113−116, which are mainly hydrophilic. Extended configurations in water or buffer folded into structures containing β-sheets in agreement with data from circular dichroism spectroscopy. In buffer, the β-sheet content was larger than in water and α−β transitions were observed at elevated temperature. β-Sheets were formed by hydrophobic residues; turns were formed by hydrophilic residues. A few typical β-sheets that contain different residues are suggested. A B18 molecule in a strand−loop−strand conformation placed in buffer in contact with vapor was spontaneously adsorbed to the buffer−vapor interface with its hydrophobic side pointing toward the vapor phase. The adsorption induced the formation of turns at positions 108−119 and α-helical conformations in the region around residues 114−117. α-Helices were parallel to the interface plane in agreement with data from IR reflection absorption spectroscopy.

Introduction

Amyloid diseases such as Alzheimer's are associated with the conversion of proteins from a soluble and functional form into a β-rich structure that often tends to precipitate in the form of fibrils. The conformational transition presumably occurs in the partially denaturing environment of a cellular compartment.[1] Addition of fluoralcohols can induce an α-helical conformation and inhibit precipitation in vitro.[2] It has been argued that the application of agents stabilizing α-helical conformation might be a therapeutic strategy against amyloid diseases.[3] Others have argued that the ability of fibrillogenic peptides to adopt α-helical structures reminiscent to that of viral fusion peptides might be in fact the origin of their toxicity.[2] In any case, for the design of specific agents against amyloid diseases, detailed knowledge about the early steps of fibrillogenesis is required. One important aspect of these early steps is the conformational behavior of fibrillogenic peptides in different environments.

Figure 1 shows the sequence of B18, a peptide with both fibrillo- and fusogenic activity. The amphiphilic and positively charged peptide is a fragment of the sea urchin fertilization protein Bindin and corresponds to residues 103−120 of the parent protein.[4] In aqueous buffer, the peptide has a pronounced tendency to precipitate in the form of amyloid-like fibrils.[5] Little secondary structure with some β-sheet content before the onset of precipitation is indicated from circular dichroism (CD) spectroscopy.[6] Addition of trifluorethanol (TFE) induces α-helical conformations.[7] A model of the peptide in a water−TFE mixture with a TFE volume fraction of 30% has been determined on the basis of NMR data.[7] In this model, the peptide forms a helix at either end, connected via a two-residue flexible loop. An α-helical conformation is also induced in bilayer stacks at low peptide-to-lipid ratio,[8] in the presence of sodium dodecyl sulfate (SDS) micelles[7] or fluorinated nanoparticles,[3] or upon adsorption to a water−vapor or buffer−vapor interface.[6]

Figure 1. Amino acid sequence of the B18 peptide, a membrane-binding and fusogenic fragment of the sea urchin fertilization protein Bindin. Top row: residue number in the parent protein. Middle row: sequence in one-letter code. Bottom row: color-coding of the sequence, distinguishing between hydrophobic residues (yellow), polar but neutral residues (blue), histidine residues (green), and arginine residues (red).

Due to the tendency of the fibrillogenic peptide to aggregate, the structure of monomers in aqueous solution on an atomic level is difficult to assess experimentally. Therefore, we have used computer simulations to compare the conformational plasticity of the peptide in different environments on a microscopic level. The B18 peptide was studied in (i) a water−TFE mixture, (ii) pure water, (iii) aqueous buffer containing 100 mM NaCl, and (iv) at a buffer−vapor interface using atomistic molecular dynamics (MD) simulations with explicit description of the solvent. The peptide was investigated as an isolated molecule in solution or at an interface. Previous MD simulations[9−13] suggest a tendency of fibrillogenic peptides to form unstructured coils or β-sheet structures in aqueous solution, and adsorption

* Email: vknecht@mpikg.mpg.de.

10.1021/jp0659204 CCC: $37.00
Published on Web 03/31/2007

TABLE 1: Different Systems Studied by MD Simulations: B18 Molecule in a Water−TFE Mixture (wat−tfe), Pure Water (wat−nmr, wat−ex, and wat−ex−hish), Aqueous Buffer Containing 100 mM NaCl (buf−nmr, buf−ex, and buf−β) or at a Buffer−Vapor Interface (ba−β and ba−nmr0)[a]

simulation	init conf	n_w	n_{TFE}	n_{Na}	n_{Cl}	box type	$a \times b \times c$ (nm^3)
wat−tfe	NMR	3600	400		2	octahedral	6.1
wat−nmr	NMR	3928			2	dodecahedral	5.6
buf−nmr	NMR	3076		6	8	cubic	$4.6 \times 4.6 \times 4.6$
wat−ex	extended	3765			2	rectangular	$8.3 \times 3.7 \times 3.8$
wat−ex−hish	extended	3764			3	rectangular	$8.3 \times 3.7 \times 3.8$
buf−ex	extended	3751		7	9	rectangular	$8.3 \times 3.7 \times 3.8$
buf−β	β	4380		8	10	rectangular	$4.8 \times 4.8 \times 20.0$
ba−β	β	3779		7	9	cubic	$5.2 \times 5.2 \times 5.2$
ba−nmr0	NMR	3088		5	6	rectangular	$4.8 \times 4.9 \times 20.0$

[a] In the simulations wat−ex−hish, His109 was modeled in a protonated state and the other histidine residues were modeled in a deprotonated state. In all other simulations, all histidine residues were modeled in a deprotonated state. The second column indicates the initial configuration chosen, corresponding to the helix−kink−helix structure of the peptide in a water−TFE mixture based on NMR data[7] (NMR), an extended configuration, or a structure containing a strand−loop−strand conformation (β) obtained from a previous simulation of the peptide in water (wat−ex). The number of water (n_w) and TFE (n_{TFE}) molecules, the number of sodium (n_{Na}) and chloride (n_{Cl}) ions, the box type, and the dimensions of the box ($a \times b \times c$) are given. Each simulation was performed three times at 293 K with different sets of initial velocities. System buf−nmr was also studied at 350 K denoted by buf−nmr, 350 K.

of a peptide or protein to a hydrophobic−hydrophilic interface can induce α-helical conformations.[14]

In MD simulations, the conformational space of the peptide is sampled by following the dynamics of the peptide in time starting from a specific initial configuration. The minimal time required to fully sample the conformational space of such a peptide may be estimated from the folding times of fast-folding peptides of this size, which is on the order of microseconds.[15] In contrast, the time scales accessible to the simulations is on the order of nanoseconds due to the high computational expense. As a consequence, the simulations can be biased by the initial conditions. Therefore, different initial structures were used. Initial structures of B18 consisted of (i) the NMR-derived helix−kink−helix conformation in a water−TFE mixture and (ii) an extended configuration (in water or buffer). The results were validated by comparison with CD data. Extended peptide configurations in water or buffer folded into strand−loop−strand structures with β-sheet contents in agreement with estimates from CD. A typical strand−loop−strand structure was used as an initial configuration in simulations of B18 in buffer in contact with vapor (modeling air). Adsorption of the peptide to the interface induced the formation of turns and α-helical conformations, supporting results from IR reflection absorption spectroscopy (IRRAS) data.

Methods

Simulation Setups. The Bindin B18 peptide was simulated in different environments in a periodic box using MD simulations. The different systems simulated are specified in Table 1 and consisted of B18 in a water−TFE mixture (wat−tfe), pure water (wat−nmr, wat−ex, and wat−ex−hish), aqueous buffer containing 100 mM NaCl (buf−nmr, buf−ex, and buf−β), and a buffer−vapor interface (ba−β and ba−nmr0). Initial configurations used were (i) the helix−kink−helix structure of B18 in the water−TFE mixture with a TFE volume fraction of 30% suggested from NMR data[7] and denoted by wat−tfe, wat−nmr, buf−nmr, and ba−nmr0 in Table 1, (ii) an extended configuration denoted by wat−ex, wat−ex−hish, and buf−ex, or (iii) a strand−loop−strand structure denoted by buf−β and ba−β. The strand−loop−strand structure contained a β-sheet consisting of the residues 106−107 and 118−119 and was obtained from the final configuration of a simulation in water (wat−ex in Table 1). The NMR structure was kindly provided by A. S. Ulrich. A missing side chain (L107) was modeled using the public domain software MolMol.[16]

For the simulations starting from the peptide in bulk solution, the protonation state of the peptide was chosen to mimic pH 7−7.5. In particular, the histidine side chains were modeled in a deprotonated state. Full deprotonation of the histidine side chains at pH 7.5 is suggested from the pK_a of isolated histidines and indicated from Hϵ_1 chemical shifts for B18 in water−TFE.[7] In pure water (pH 7), each of the three histidines undergoes transitions between different protonation states. Assuming the pK_a of each of these histidines to be equal to the pK_a 6.0 of isolated histidines, the ratio of the populations of the protonated and the deprotonated state of a histidine is about 1:10. To study the qualitative effect of the protonation of a histidine, we performed also simulations in which His109 was modeled in a protonated state denoted by wat−ex−hish. The protonation state of the peptide at the buffer−vapor interface (ba−nmr0) was chosen such as to mimic an increased local pH at the interface suggested from disjoining pressure experiments.[17] At a bulk pH of 7−7.5, the density of hydroxyl ions per interfacial area has been estimated to be 2.6×10^{-8} mol m^{-2}.[17] For an interface thickness of 1 nm suggested from MD simulations,[18] this corresponds to a local pH of 12.4. Assuming the pK_a of the N-terminal leucine residue to be similar to the pK_a 9.6 of isolated leucine residues, the N-terminus was modeled in a deprotonated state.

The initial configurations of the simulations were chosen as follows. The peptide was placed in a periodic box with a minimal distance of 1.3 nm between the peptide and the boundaries of the box. In the case of the system wat−tfe (compare Table 1), TFE molecules were randomly distributed. The remaining space was filled with water molecules. Chloride ions were added to counterbalance the positive charge of the peptide. For the systems buf−nmr, buf−ex, buf−β, ba−β, and ba−nmr0 as described in Table 1, selected water molecules were replaced by sodium or chloride ions to mimic 100 mM NaCl. For the simulations of B18 at a buffer−vapor interface, the interface was created by first filling a cubic or quasi-cubic box of 4.8 nm edge length with water. Subsequently, the box was extended in the z direction (parallel to c; see Table 1) to effectively remove the periodicity of the box in this dimension and to obtain an air phase modeled as vapor. The peptide was either placed in the bulk water corresponding to ba−β in Table 1, or at an interface denoted by ba−nmr0 in Table 1. Water molecules overlapping with the peptide were removed, and ions were added as described. Each system was minimized using steepest descent to remove residual overlaps of atoms. The

solvent was equilibrated in a subsequent simulation of 1 ns, restraining the atoms of the peptide close to their initial positions by using a harmonic potential. Finally, each system was simulated three times for 50 ns using different sets of initial velocities.

The peptide was described using the GROMOS96-43a1 force field[19] in which CH_i groups ($i = 1, 2, 3$) are described using united atoms. Water molecules were represented by the three-site simple point charge (SPC) model.[20] All simulations were performed using the GROMACS[21] simulation code. The covalent bond lengths were constrained using the LINCS[22] (peptide) or SETTLE method[22] (water molecules), respectively. In addition, the masses of atoms attached to hydrogens were redistributed so as to increase the mass of the hydrogen atoms simulated explicitly. This eliminates high-frequency motions of the hydrogens, which allows the use of a time step of 4 fs.[23] Even though this slightly alters the kinetic properties of the system, it does not affect its structural properties. It has been found that even 5 fs time steps did not affect the populations of alternative conformational states of peptides significantly.[24] The temperature was kept constant at 293 K in agreement with the experimental conditions by separately coupling the peptide and the solvent to an external temperature bath.[25] In the simulations of the peptide in bulk water, the pressure was kept constant at 1 bar by rescaling the box size.[25] Fixed box dimensions were used for the simulations of the buffer−vapor interface. Full electrostatic interactions were computed using the particle mesh Ewald technique[26] with tinfoil boundary conditions.[27] Snapshots were saved every 20 ps for further analysis.

Analysis. The secondary structure of the peptide was determined on the basis of an analysis of hydrogen bonds within the main chain of the peptide according to the following definitions.[28] An *n*-turn is characterized by a hydrogen bond between residues i and $i + n$. A 3-turn is also called β-turn. Two or more consecutive *n*-turns form an *n*-helix. The case $n = 4$ indicates an α-helix, $n = 3$ a 3_{10}-helix, and $n = 5$ a π-helix. Two strands joined by hydrogen bonds involving alternating residues on each participating strand indicate a β-sheet, if each strand contains two or more residues, or a β-bridge, if each strand contains only a single residue. A strongly curved region in the peptide backbone is called a bend. Regions showing neither of these secondary structure motifs are denoted as coil. The content of selected secondary structure motifs of the peptide was determined by averaging over the final 20 ns of the simulations. Here, the α- and π-helical content, the β-sheet, turn, and bend content were considered. To compare to data from CD spectroscopy,[29,30] also the total helical content, the turn−bend content corresponding to the sum of the turn and the bend content, and the sum of the coil and the β-bridge content, representing the unstructured peptide segments, were considered. For some of the simulations, the α-helical, β-sheet, and turn contents per residue were determined. Error bars were obtained by calculating the standard error of the estimates from three independent simulations using different initial velocity distributions.

As a measure for the compactness of a peptide configuration, the radius of gyration, R_g, defined as

$$R_g = \left(\frac{\sum_i ||r_i||^2 m_i}{\sum_i m_i} \right)^2 \quad (1)$$

was calculated for some of the simulations. Here, m_i is the mass of atom i, and r_i is the position of atom i with respect to the center of mass of the molecule. Main chain hydrogen bonds were counted using a geometrical cutoff criterion for the existence of a hydrogen bond. A hydrogen bond was defined to exist when (i) the distance between donor and acceptor was less or equal to 0.35 nm, and (ii) the angle between the vectors connecting the donor and the hydrogen or acceptor, respectively, was less or equal to 60°. As a measure for the degree to which nonpolar groups of the peptide are exposed to the solvent for a given peptide configuration, the hydrophobic solvent accessible surface area (SASA) of the peptide was calculated. The hydrophobic SASA of a solute is the area traced out by the center of a probe sphere representing a water molecule as it is rolled over the nonpolar groups of the solute. The SASA was calculated on the basis of an algorithm by Connolly[31] using the program g_sas from the GROMACS package.[21]

Results

Simulations were started from the helix−kink−helix structure of B18 in water−TFE with a TFE fraction of 30 vol % suggested from NMR data[7] (B18 in water−TFE, pure water, buffer, and the buffer−vapor interface), from an extended configuration (B18 in water and buffer), or a strand−loop−strand structure previously formed in bulk water (B18 in bulk buffer and buffer in contact with vapor). The three histidines were modeled in a deprotonated state to mimic pH 7−7.5. At the interface, the N-terminus of the peptide was modeled in a deprotonated state to mimic an increased interfacial pH of 12.4. The simulations were performed at 293 K to mimic experimental conditions. Simulations of B18 in buffer starting from the helix−kink−helix structure were also performed at 350 K to facilitate the crossing of high-energy barriers. Each type of simulation, characterized by the environment, the initial configuration of the peptide, and the temperature, was performed three times with different sets of initial velocities. Each simulation covered a time period of 50 ns. The total simulated time was about 2 μs. The final 20 ns of each simulation were used for analysis.

The secondary structure content observed in the simulations was compared against estimates from CD data shown in Table 2 (CD). Note that secondary structure analyses based on CD data do not distinguish between different helix types but give the overall helical content that is assumed to be close to the α-helical content due to the abundance of this helix type in known protein structures. Other secondary structure motifs probed by CD are the β-sheet content, the sum of the turn and bend content (turn−bend content), and the unstructured content (sum of the coil and β-bridge content).[29,30] In the analyses of the simulations, the content of the secondary structure motif classes probed by CD and single secondary structure motifs were determined.

The Stability of Preformed α-Helical Conformation Depends on the Environment. The simulations suggest that the conformational behavior of the peptide is strongly dependent on the environment in agreement with experimental data. Table 2 gives estimates for the secondary structure content of the peptide at different conditions from simulations and experiment.[6,7] In general, averaged over all amino acids of the peptide and over time, large portions of the peptide (28−56%) were unstructured. As shown in Table 2 (method MD^H), the preformed helical conformation was more stable in the buffer−vapor interface (ba−nmr0, 57 ± 10%) and in the water−TFE mixture (wat−tfe, 43 ± 7%) than in bulk water (wat−nmr, 29 ± 1%) or bulk buffer (buf−nmr, 33 ± 8%). The helix-stabilizing effect of TFE and the buffer−vapor interface is in qualitative agreement with data from CD shown in Table 2 (CD, water−

TABLE 2: Contents of Secondary Structure Motifs (%) for B18 in Molecular Dynamics (MD) Simulations of the Peptide in a Water−TFE Mixture with an Effective Volume Fraction of TFE in the Bulk between 14 and 30% (wat−tfe), Pure Water (wat−nmr, wat−ex, and wat−ex−hish), Aqueous Buffer Containing 100 mM NaCl (buf−nmr, buf−ex, buf−β, and buf−nmr, 350 K), and at a Buffer−Vapor Interface (ba−β and ba−nmr0)[a]

method	sim/sys	helix	α	π	β	t + b	turn	bend	unstr
MD^H	wat−tfe	43 ± 7	40 ± 8	3 ± 3	0	12 ± 4	6 ± 3	6 ± 2	39 ± 5
MD^H	wat−nmr	29 ± 1	11 ± 4	18 ± 3	0	21 ± 6	11 ± 3	10 ± 4	32 ± 5
MD^H	buf−nmr	33 ± 8	20 ± 6	13 ± 6	0	28 ± 2	15 ± 3	13 ± 4	39 ± 6
MD^H	ba−nmr0	57 ± 10	51 ± 13	6 ± 4	0	14 ± 5	5 ± 3	9 ± 5	28 ± 5
MD^E	wat−ex	0	0	0	10 ± 2	34 ± 1	10 ± 3	23 ± 3	56 ± 2
MD^E	wat−ex−hish	0	0	0	26 ± 16	20 ± 4	3 ± 2	17 ± 5	54 ± 18
MD^E	buf−ex	0	0	0	27 ± 13	27 ± 3	5 ± 4	22 ± 5	46 ± 10
MD^β	buf−β	0	0	0	16 ± 4	31 ± 3	4 ± 1	27 ± 2	53 ± 2
MD^β	ba−β	9 ± 4	7 ± 4	0	7 ± 4	36 ± 4	10 ± 4	26	48 ± 4
MD^T	bn, 350 K	4 ± 3	3 ± 3	1 ± 1	27 ± 13	27 ± 4	7 ± 3	20 ± 3	42 ± 7
CD (7)	water−TFE	24 ± 16							
CD (6)	water	8 ± 6			12 ± 12	12 ± 2			69 ± 5
CD (6)	buffer	4 ± 3			32 ± 17	17 ± 7			53 ± 15

[a] Simulations denoted by MD^T were performed at 350 K. All other simulations were performed at 293 K. Simulations were started from a predominantly α-helical (MD^H and MD^T/bn, 350 K), an extended (MD^E), or a strand−loop−strand structure (MD^β). The simulation setups are specified in Table 1. Helix denotes the total helical content, α or π the α- or π-helical content, β the β-sheet content, t + b the sum of the turn and the bend content, and unstr the unstructured content. The numbers give the average value and standard error from the final 20 of three independent 50 ns simulations. Experimental estimates based on CD data[6,7] for the secondary structure content of the peptide in a water−TFE mixture with a volume fraction of TFE between 14 and 30% (water/TFE) and water at pH 7 (water); aqueous buffer at pH 7.5 and [NaCl] = 100 mM (buffer) are also given. Ranges of experimental estimates indicate the scattering of estimates arising from sample preparation and the method used to estimate the structure content from the spectra (CD, water, and buffer)[6] or from the uncertainty of the effective concentration of the cosolvent (CD, water−TFE).

tfe, water, and buffer) and IR reflection absorption spectroscopy (IRRAS).[6] The effect of the environment on the stability was even more pronounced for the α-helical conformation. The α-helical conformation was most stable in the buffer−vapor interface (ba−nmr0, 51 ± 13%), somewhat lower in the water−TFE mixture (wat−tfe, 40 ± 7%), lower in buffer (buf−nmr, 20 ± 6), and lowest in pure water (wat−nmr, 11 ± 1).

Stability of α-Helical Conformation in Water−TFE Mixture. A quantitative comparison of the total helical content of the peptide in the water−TFE mixture with experimental data is not straightforward. This is because (i) the helical content of the peptide depends sensitively on the TFE concentration, (ii) TFE is inhomogeneously distributed around the peptide, (iii) the peptide concentration in the simulations is about 2 orders of magnitude larger than in the experiments,[7] and (iv) the adsorption of TFE molecules to the peptide is presumably enhanced compared with the experiment. For a perfect TFE model, which gives the correct distribution, the concentration of TFE in the bulk of the simulation box would have to be equal to the average concentration of TFE in the experiment. The average TFE concentration in the simulation box was chosen to be 0.11 TFE molecules per water molecule, corresponding to 30 vol %. To determine the bulk concentration of TFE in the simulations, the local number of TFE molecules per water molecule was determined as a function of the distance from the center of mass of the peptide. As shown in Figure 2a,b, TFE is highly enriched close to the peptide, with a maximal local concentration of 5.2 TFE per water molecule. This adsorption of TFE onto the peptide, which was also observed in previous simulations, has been suggested to be part of the mechanism by which TFE stabilizes α-helical conformations.[32] In the bulk, TFE is depleted down to 0.05 TFE molecules per water molecule, corresponding to a TFE volume fraction of 14%. However, a value of 14% is likely to underestimate the effective TFE concentration because of inaccuracies of the TFE model. The conformational behavior of the peptide is expected to be determined by the local TFE concentration around the peptide. As the mixing enthalpy of TFE and water is too unfavorable in the simulations compared to experiment,[33] the TFE will tend to complex more favorably with the hydrophobic residues of the peptide. This, combined with a 100-fold higher concentration of the peptide in solution compared with experiment, will cause the bulk-deletion effect of TFE to be overestimated. Therefore, for a local TFE concentration of about 5 TFE per water molecules close to the peptide as observed in the simulations, the TFE concentration in the bulk is likely to be larger than observed in the simulations with an upper bound of 30 vol %. These considerations suggest that the effective TFE concentration of the simulations is between 14 and 30 vol %. An experimental estimate for the helical content at a given volume fraction of TFE may be obtained from the respective amplitude of the ellipticity measured by CD at 222 nm and linear interpolation between zero and the amplitude expected for a full helix.[7] For the range of effective TFE concentrations studied here, a helical content between 18% and 50% is thus expected. The helical content observed in the simulations is within the expected range. The average α-helical content per residue in water−TFE is shown in Figure 3a. The α-helical conformation is found to be more stable in the peptide segment containing the C-terminal than in the one adjacent to the N-terminal and correlates with the hydrophilicity of the local amino acid sequence, being most stable at positions 113−117.

Stability of α-Helical Conformation in Water or Buffer. The presence of some helical content in water as given in Table 2 (wat−nmr) is in qualitative agreement with experiment (CD, water). The average α-helical content per residue is shown in Figure 4a. Again, the helicity correlates with the hydrophilicity

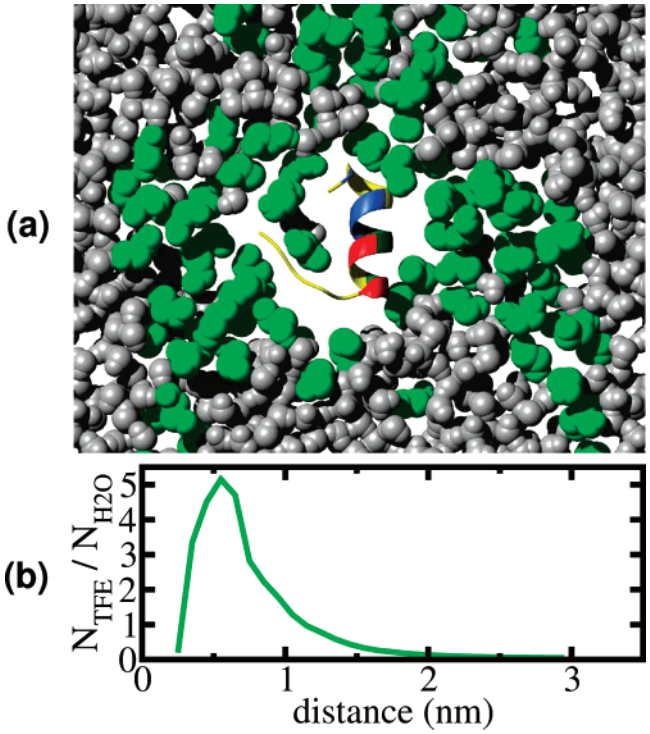

Figure 2. Adsorption of TFE to B18 in a water−TFE mixture with an average volume fraction of TFE of 30%. (a) Configuration after 50 ns of simulation. The backbone of the peptide is shown in ribbon representation, with the amino acid sequence color-coded similar to Figure 1. TFE (green) and water molecules (gray) are shown in space-filling representation. The figure only shows molecules whose center of mass lies within a slab of 1.2 nm thickness. The figure was prepared using the public domain software MolMol[16] and POV-Ray.[34] (b) Distribution of TFE during the final 20 of a 50 ns simulation. The average number N_{TFE} of TFE molecules per water molecule as a function of the distance from the center of mass of the peptide is shown. The TFE distribution exhibits a narrow peak in the vicinity of the peptide, indicating that TFE is adsorbed to the peptide. The TFE volume fraction in the bulk was 14%.

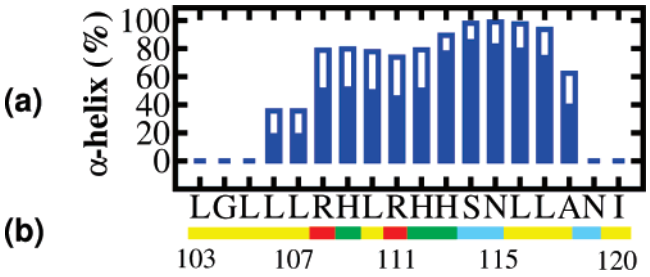

Figure 3. Helicity of B18 in a water−TFE mixture with an average volume fraction of TFE of 30%. Three 50 ns simulations were performed starting from the same helix−kink−helix structure from ref 7 but three different initial velocity distributions. (a) Average α-helical content per residue during the final 20 ns of the three simulations. The filled bars represent average values; the open bars indicate the standard error. (b) Amino acid sequence of the peptide shown using a representation as explained in Figure 1.

of the local sequence. Significant α-helical content (>20%) is found for residues 112−117.

As evident from Table 2, the absolute amount of helical conformation in water (wat−nmr) or buffer (buf−nmr) is larger than experimental estimates (CD, water and CD, buffer). In addition, a high percentage of π-helical conformation was formed both in water (wat−nmr, 36 ± 8%) and in buffer (buf−nmr, 24 ± 4%). π-Helices are extremely rare in known protein structures but can occur as intermediates in α-helix−coil

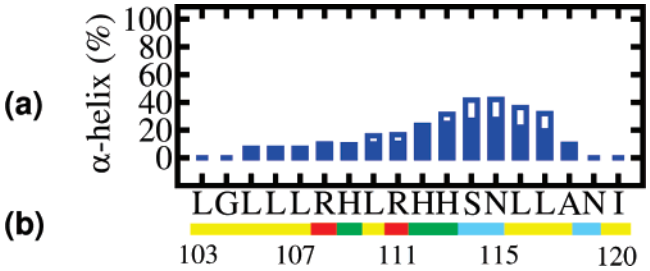

Figure 4. (a) Average α-helix content per residue during the final 20 ns of the three simulations of B18 in water started from a helix−kink−helix structure.[7] (b) Amino acid sequence of the peptide shown using a representation as explained in Figure 1.

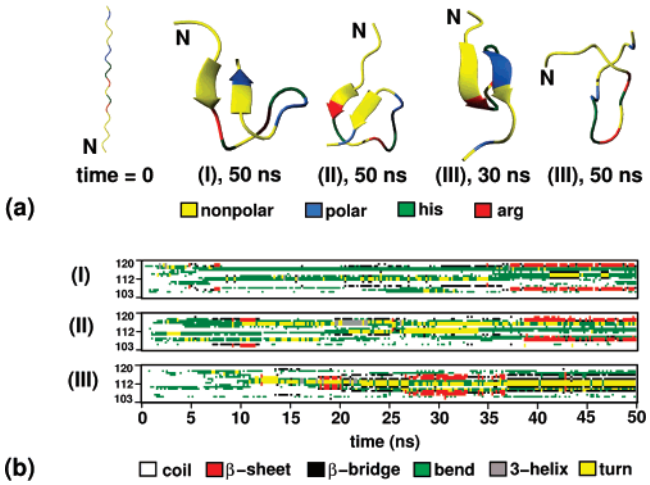

Figure 5. Formation of β-sheets for Bindin B18 peptide in water at 293 K. Three 50 ns simulations were performed starting from the same extended configuration as shown in (a, time = 0) but for different initial velocity distributions (I, II, and III). (a) Initial (time = 0), final (I−III, 50 ns), and intermediate configurations (III, 30 ns) shown in a representation similar to that chosen in Figure 2a. (b) Time evolution of the secondary structure of the peptide for the three different sets of initial velocities as obtained from the analysis of hydrogen bonds in the peptide main chain using the program DSSP.[28] Here, the vertical coordinate represents the residue number which is plotted against time, and the secondary structure is color-coded.

transitions as suggested in a previous MD study.[35] In our simulations of B18 in water or buffer, π-helical conformation was formed from the α-helical conformation and either converted into a coil or was (meta)stable on the time scale of the simulations (data not shown). β-Sheets were neither formed in water nor in buffer, although significant β-sheet content in buffer is indicated from CD. The overrepresentation of helical conformation compared to experiment, the high π-helical content, and the absence of β-sheet content indicate that the conformation of the peptide was kinetically trapped in regions close to the initial α-helical conformation. To remove this bias from the initial conformation, further simulations were carried out starting from an extended configuration.

Formation of β-Sheets in Water. Figure 5 shows the results of simulations of the peptide in water starting from an extended peptide configuration (a, time = 0). During the simulations, small β-sheets (b, I−III, red), turns (b, I−III, yellow), and bends (b, I−III, green) formed. As shown in Table 2 (wat−ex), the average β-sheet content (10 ± 2%) was consistent with estimates from CD for B18 in water (CD, water). The turn−bend content (34 ± 2%) was a factor of 3 larger than estimates of the turn−bend content of B18 in water from CD (CD, water). It should be noted here that direct comparison of the simulations with

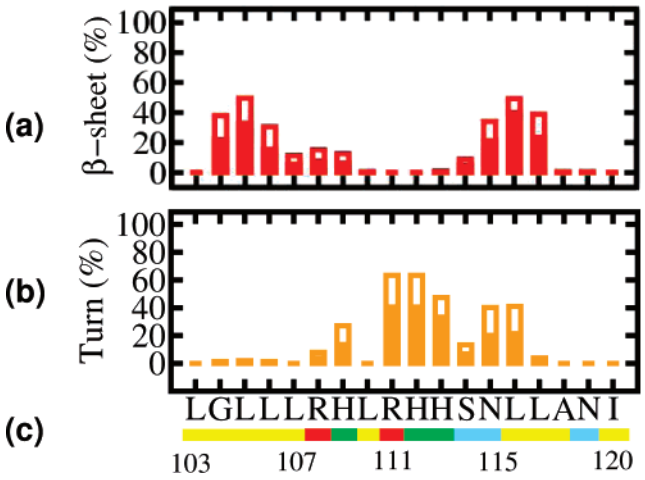

Figure 6. Average β-sheet (a) and turn content (b) of B18 in water in simulations starting from an extended configuration of the peptide as shown in Figure 5. The representation is as in Figure 3.

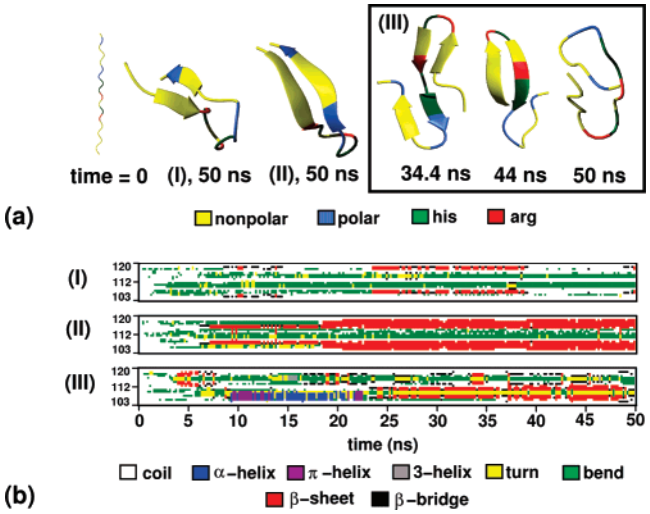

Figure 7. Increased formation of β-sheets for B18 in aqueous buffer containing 100 mM NaCl at 293 K. Three 50 ns simulations were performed starting from the same extended initial configuration of the peptide shown in (a, time = 0) but for different initial velocity distributions (I, II, and III). The representation is the same as in Figure 5.

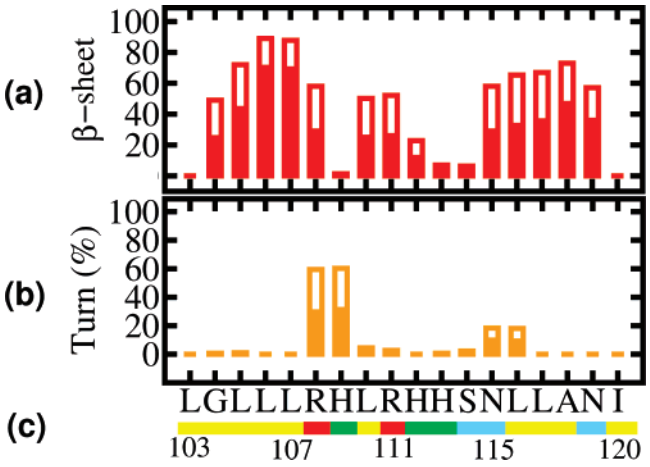

Figure 8. Average β-sheet (a) and turn content (b) of B18 in buffer in the simulations shown in Figure 7 starting from an extended peptide configuration. (c) Amino acid sequence of the peptide. The representation is the same as in Figures 3 and 6.

CD spectra is difficult. Relating intensities to percentage of secondary structure is context dependent. The parameters used to relate signal intensity to structure have been fitted to proteins[36,37] and may not be fully applicable to short peptides.[13]

A difference between the secondary structure of the peptide in experiment and in the simulation might arise from a difference in (i) the effective acidity and (ii) the ionic strength between the simulations and experiment: (i) In water (pH 7), each of the three histidines undergoes transitions between different protonation states. From the pK_a 6.0 of isolated histidines, the ratio of the populations of the protonated and the deprotonated state of a histidine is estimated to be about 1:10. This was approximated by modeling each histidine in a deprotonated state, neglecting the contribution of the partially occupied protonated state on the conformational behavior of the peptide. (ii) Due to the artificially high concentration of peptide combined with the counter-ions necessary for charge neutralization, the effective ion concentration was higher than in experiment. To study the qualitative effect of the protonation of histidine residues, simulations were also performed in which His109 was modeled in a protonated state. As shown in Table 2 (wat−ex−hish), the turn−bend content was decreased (20 ± 4, %) and thus closer to the experimental estimate for B18 at pH 7. The β-sheet content was increased (26 ± 13%).

Figure 6 shows the average β-sheet (a) and turn content (b) per residue in the simulations in which all histidine residues were taken to be deprotonated (wat−ex). Turns were mainly formed by hydrophilic residues, including residues 111−113 (sequence RHH) with more than 30% turn content. β-Sheets were mainly formed by hydrophobic residues, suggesting a stabilization of β-sheets by hydrophobic interactions. Residues with more than 20% β-sheet (106−108, 117−119) included three leucine residues (positions 106, 107, 117). Leucines are found to have a high propensity to form β-sheets in known protein structures.[38] For leucines 106, 110, and 117, β-sheet structure is suggested from NMR data on B18 in phospholipid bilayer stacks at high peptide-to-lipid ratio.[39] As shown in Figure 5a (I, 50 ns), an antiparallel β-sheet was formed between residues 106−107 and 118−119. Parallel β-sheets were formed between residues 110−111 and 117−118 (Figure 5a, II, 50 ns) or 106−108 and 114−116 (a, III, 30 ns).

Increased β-Sheet Content in the Presence of Sodium Chloride. Figure 7 shows the results of simulations of the peptide in buffer containing 100 mM NaCl. Again, an extended conformation was used as initial configuration of the peptide (Figure 7a, time = 0), and β-sheets, turns, and bends formed during each of the three simulations. As shown in Figure 7b (III), a helical intermediate with α- and π-helical conformation in the N-terminal segment and 3_{10}-helical conformation in the C-terminal segment formed in one of the simulations. No helical intermediates were observed in the other simulations (Figure 7b (I−II)). As shown in Table 2 (MD^E, buf−ex), the average β-sheet (27 ± 13%), turn−bend (27 ± 3%), and unstructured content (46 ± 10%) were in agreement with estimates from CD (Table 2, CD, buffer). The β-sheet content was larger than in pure water (MD^E, wat−ex), in agreement with experiment (Table 2, CD, buffer, and water). The major component of the turn−bend content was the bend content (22 ± 5%). The average β-sheet and turn content per residue is shown in Figure 8. Similar to pure water, β-sheets were mainly formed by hydrophobic residues (Figure 8a), and turns were primarily formed by hydrophilic residues (b). The largest β-sheet content (about 70%) was found for the leucine residues 106 and 107. Again, an antiparallel β-sheet was formed between residues 106−107 and 118−119 (Figure 7a, I, 50 ns). Further antiparallel β-sheets were observed between residues 104−108 and 115−

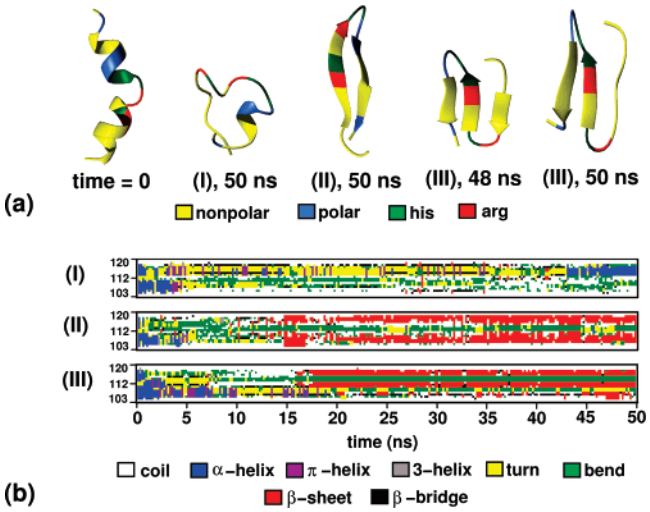

Figure 9. α−β-Transitions of B18 in aqueous buffer containing 100 mM NaCl at 350 K. Three 50 ns simulations were performed starting from the same extended configuration as shown in (a, time = 0) but for different initial velocity distributions (I, II, and III). The representation is the same as in Figures 5 and 7.

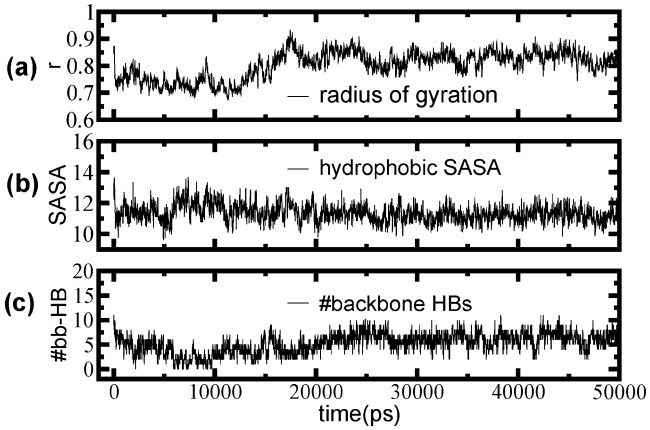

Figure 10. Time evolution of (a) the radius of gyration, (b) hydrophobic solvent accessible area, and (c) number of main chain hydrogen bonds, during an α−β-transition of B18 in buffer (simulation II shown in Figure 9).

119 (II, 50 ns) or 106−107 and 110−111 (III, 34.4 ns) (lower β-sheet). An antiparallel β-sheet was also formed between residues 104−107 and 110−113 (III, 44 ns). These β-strands were connected by a two-residue turn (consisting of R108 and H109), with R108 predominantly forming backbone dihedral angles $\phi = 60 \pm 20°$ and $\psi = -85 \pm 25°$. The residues 104−113 thus formed a type II′ β-hairpin.

As shown in Table 2 (MD^E, wat−ex, and buf−ex), no α-helical conformation was observed during the final 20 ns of the simulations of B18 in water or buffer starting from an extended configuration, although small amounts of α-helical structure are indicated from CD data (Table 2 CD, water, and buffer). This suggests a bias arising from the initial extended structure, complementary to the bias from the preformed helical conformation described above. Nevertheless, the simulations using different initial conditions yield useful complementary information. The simulations starting from an extended configuration reveal residues with high propensity to form β-sheets or turns; the simulations starting from the preformed α-helical conformation suggest residues with high α-helix propensity. β-Sheets are formed by hydrophobic residues; turns or α-helices are formed by hydrophilic residues.

α-β-Transitions in Buffer at Elevated Temperature. As shown in Table 2 (CD, buffer), CD data indicate significant β-sheet, but low α-helical, content for B18 in buffer. β-Sheets were formed in the simulations starting from an extended peptide configuration (Table 2, buf−ex, and Figure 7) but not in the simulations starting from a preformed α-helical conformation (Table 2, buf−nmr). This suggests that preformed α-helical conformations were kinetically trapped in a local free energy minimum due to high-energy barriers involved in conformational transitions. To facilitate the crossing of energy barriers, simulations at elevated temperature were performed. Figure 9 shows results from simulations of B18 in buffer using the helix−kink−helix structure as initial configuration (a, time = 0) and choosing a temperature of 350 K. In three independent simulations, the initial α-helical conformation dissolved rapidly (within about 10 ns) (Figure 9b), and (meta)stable β-sheets formed after about 15 ns (Figure 9b, II and III).

As shown in Table 2 (bn, 350 K), the overall β-sheet (27 ± 13%), turn−bend (27 ± 4%), and unstructured content (47 ± 2%) were similar to that formed in simulations with extended initial peptide configurations at 293 K (buf−ex). As shown in Figure 9a, antiparallel β-sheets were formed between residues 106−111 and 115−119 (a, II, 50 ns) or 110−112 and 116−118 (a, III, 48 ns) (left β-sheet). Again, a type II′ β-hairpin was formed by the residues 104−113 (a, III, 48 ns) (right β-sheet). In one of the simulations (Figure 9a, I, 50 ns; b, I), residues 113−117 refolded into an α-helical conformation. Taken together, the simulations at elevated temperature support the high propensity of B18 to form β-sheets in buffer and suggest typical β-sheets.

The α−β−transitions observed at elevated temperature may mimic the kinetics of conformational transitions upon a change of the solvent environment; therefore, the kinetics of this process shall be discussed somewhat more in detail. Figure 10 shows the evolution of (a) the radius of gyration, (b) the hydrophobic solvent accessible surface area, and (c) the number of main chain hydrogen bonds of the peptide in simulation II shown in Figure 9 in which an extended β-sheet was formed. Dissolution of α-helical conformations was accompanied by a quick decrease in the radius of gyration (Figure 10a), indicating the peptide to adopt more compact structures. A concomitant decrease of the hydrophobic SASA of the peptide (Figure 10b) suggests this collapse to be driven by the hydrophobic effect. A similar hydrophobic collapse prior to β-sheet formation was also observed in simulation III shown in Figure 9. As shown in Figure 9b, α-helical conformations converted into π-helical conformations and single turns. Turns typically dissolved into bend and, subsequently, more extended conformations, before β-sheets were formed. The dissolution of helical and turn conformations resulted in a decrease in the number of intramolecular hydrogen bonds, which increased again upon β-sheet formation (Figure 10c). These results suggest a two-step mechanism for α−β-transitions in B18: In step one, α-helical conformations dissolve into more compact, barely structured intermediates (α−coil transition). In step two, the coil intermediates reorganize into more ordered β-sheet structures (coil−β transition). Compact coil intermediates were also reported previously for α−β-transitions of fibrillogenic peptides with other sequences in simulations using simplified[40] or atomistic models.[9,41] Analogous to the initial hydrophobic collapse in α−β-conformational transitions in monomers, other simulation studies suggest the formation of hydrophobic contacts to precede β-sheet hydrogen bond formation also during aggregation of fibrillogenic peptides.[42,43]

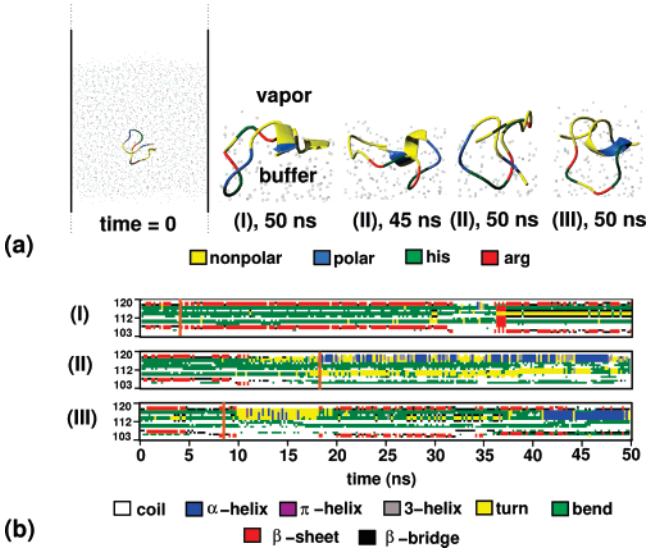

Figure 11. Adsorption of B18 to a buffer−vapor interface at 293 K. Three 50 ns simulations were performed using the strand−loop−strand structure shown in Figure 5a (I, 50 ns) as initial peptide configuration but different initial velocity distributions (I, II, and III). The representation is similar to that chosen in the Figures 5, 7, and 9. In part a, the oxygen atoms of the water molecules are shown as small, gray spheres. They are included here in order to indicate the interfacial position of the peptide. In part a (time = 0), the simulation box is indicated by black bars to indicate the position of the interface. In part b, the time of adsorption determined by the distance of the peptide to the interface is indicated by brown bars.

Adsorption of B18 at Buffer−Vapor Interface. To study the initial steps of the adsorption of B18 to a buffer−vapor interface, a B18 molecule was placed in a slab of buffer in contact with vapor (Figure 11a, time = 0). The initial peptide configuration was obtained from a previous simulation of B18 in bulk water and contained an antiparallel β-sheet consisting of the residues 106−107 and 118−119 as shown in Figure 5a (I, 50 ns). We note that a similar structure was also formed in buffer (Figure 7a, I, 50 ns). The same initial configuration was also used in simulations of B18 in bulk buffer in the absence of an interface for comparison. In the presence of an interface, the peptide was adsorbed to the interface within 15 ns (Figure 11b, I−III) (brown bars). The hydrophobic side pointed toward the vapor phase as shown in Figure 11a (I−III, 50 ns and II, 45 ns). The peptide was in immediate contact with the vapor phase. These observations support the view that the adsorption is driven by the hydrophobic effect. As shown in Table 2 (MD^E), the average β-sheet content was decreased from 16 ± 4% in bulk buffer (buf−β) to 7 ± 4% at the interface (ba−β). At the interface, an average α-helical content of 7 (±4)% was observed, in contrast to the simulation in bulk buffer (ba−β) where no α-helical conformation was formed. The average turn content was increased from 4 (±1)% in the bulk to 10 (±4)% at the interface. Turns were formed at positions 108−119. Turn formation preceded α-helix nucleation at positions 113−117 (Figure 11b, III) or fast transitions between 3_{10}-helical and α-helical conformations and turns at residues 114−119 (Figure 11b, II). These results are in agreement with a previous MD study suggesting that α-helix nucleation is preceded by the formation of either a β-turn or a 3_{10}-helix.[44] Some 3_{10}-helical conformation was observed at residues 113−117 in our simulations of B18 in the water−TFE mixture. A low, but significant 3_{10}-helix propensity of residues 115−118 is indicated from NMR data for B18 in water−TFE with a TFE fraction of 30 vol %.[7] An intrinsic 3_{10}-helix propensity of residues 113−118 may facilitate α-helix nucleation in this region.

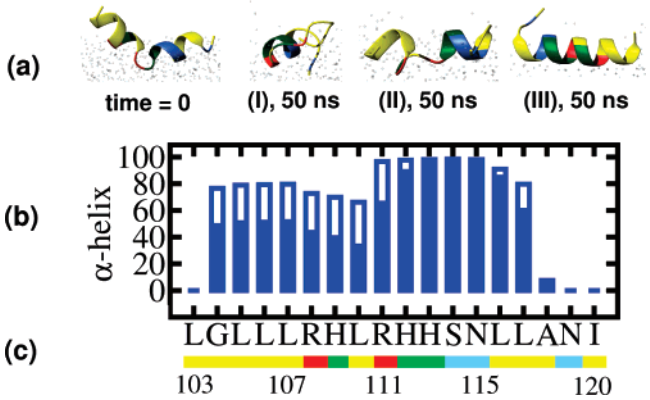

Figure 12. Conformational behavior of B18 in a buffer−vapor interface. Three 50 ns simulations were performed using the same helix−kink−helix structure shown in part a (time = 0) as initial peptide configuration but different initial velocity distributions (I, II, and III). (a, I−III, 50 ns) final configurations. (b) Average α-helical content per residue. (c) Amino acid sequence of the peptide. The representation is as in Figures 3 and 11.

Figure 12 shows the results of simulations of B18 at a buffer−vapor interface starting from the helix−kink−helix structure at the interface (a, time = 0). The average α-helical content of the peptide in these simulations was discussed above. The peptide was oriented such that its hydrophobic side pointed toward the vapor phase, consistent with the spontaneous orientation adopted upon adsorption. Figure 12a (I−III, 50 ns) shows the final configurations. The two initial α-helices either partially dissolved (a, I−II) or merged into a single continuous helix (a, III). The average α-helical content per residue is shown in Figure 12b. α-Helical conformation was most stable at positions 112−116. The overall α-helical content was 51 ± 13% and thus higher than in simulations of B18 in water, buffer, or the water−TFE mixture using the same initial configuration (Table 2). The helix axes were oriented parallel to the interface. The partial α-helical conformation of the peptide and the in-plane orientation of helix axes are in agreement with IRRAS data.[6]

Discussion

For B18, preformed α-helical conformations were more stable than for other fibrillogenic peptides of similar length in previous simulation studies.[9,13] For the amyloid forming peptides Aβ-(12−28) and PrP106−126 associated with Alzheimer's[9] or Prion diseases,[9,13] respectively, preformed α-helical conformations typically dissolved within 10 ns at 300 K. For PrP106−126 at 300 K, α−β-transitions were observed on a nanosecond time scale. In contrast, no α−β-transitions were observed for B18 at 293 K in water or buffer on a total simulated time scale of 300 ns, although low α-helical content, but significant β-sheet conformation, in this environment is indicated from CD data. Nevertheless, α−β-transitions were observed at 350 K, indicating that preformed α-helical conformations were kinetically trapped on the nanosecond time scale of the simulations at room temperature. The metastability of preformed α-helical conformations may indicate a higher intrinsic α-helix propensity for B18. Despite the metastability of preformed α-helical conformations, the α-helix-destabilizing effect of water or buffer versus a water−TFE mixture or a buffer−vapor interface was reproduced qualitatively, and residues with high or low α-helix propensity were identified.

In general, kinetic trapping is observed if a structure is in a (local) free energy minimum, which is likely the case for the helix−kink−helix structure of B18 in water−TFE (30:70) (v,v) used as initial conformation for some of the simulations. An extended structure, instead, is presumably energetically unfavorable. Accordingly, in simulations using an extended initial configuration, β-sheets and turns were formed in quantitative agreement with estimates from CD data. Different β-sheets consisting of different residues were observed. A principal conformation, i.e., folded structure, however, is not evident from the data. This either means that such a conformation does not exist for B18 in the environments studied or that the accessible time scales are too short for convergence of the simulations in terms of a principle peptide conformation. As noted in the Introduction, the folding times of peptides of this size are on the order of milliseconds or longer and thus exceed the time scales accessible to atomistic MD simulations with explicit solvent by several orders of magnitude. Nevertheless, the simulations do show convergence in terms of the content of given secondary structure motifs along the peptide sequence. In water of buffer, some β-sheets formed twice in independent simulations, suggesting them to be typical structures in these environments or important folding intermediates.

In water or buffer, β-sheets were predominantly formed by hydrophobic residues. In all environments, α-helical and turn conformations were predominantly formed by or more stable for hydrophilic segments. Similar properties, a correlation (i) between the hydrophilicity of the local peptide sequence and the stability of α-helical conformation and (ii) between the hydrophobicity of the local peptide sequence and the β-sheet propensity, have been observed in previous simulation studies for other fibrillogenic peptides.[11,13,45,46] Such a correlation is also observed experimentally for the amyloid(A)β (25−35) peptide, a fragment of the Aβ (1−42) associated with Alzheimer's disease. High-resolution structures of this peptide in mixtures of water and fluoralcohol hexafluorisopropanol (HFIP) with two different volume fractions have been determined using NMR data.[47] For a HFIP volume fraction of 80%, the peptide shows α-helical and turn conformations over its full length. For a HFIP volume fraction of 20%, the peptide only forms a single turn in the N-terminal segment that is hydrophilic, whereas the C-terminal segment that is hydrophobic adopts an (β-strand-like) extended conformation. A tendency of hydrophobic or hydrophilic residues to form β-sheet or α-helical conformations, respectively, may be explained from a side-chain specific screening of local and nonlocal electrostatic interactions of main chain polar atoms.[48]

Our simulations suggest a high propensity of B18 to form unstructured coils or strand−loop−strand structures in water or aqueous buffer. This is similar to what has been found for other fibril-forming peptides in previous simulation studies,[9,13,41] in particular, for the peptide Aβ (10−35). This peptide is a fragment of the amyloid β (Aβ) (1 − 42) peptide associated with Alzheimer's disease and adopts a collapsed coil in water as inferred from solution NMR data.[49] Previous MD simulations suggest this collapsed coil to be in exchange with strand−loop−strand structures, which are considerably populated at conditions shown to promote fibril formation.[10] The U-shaped topology of a strand−loop−strand structure is similar to the topology of Aβ (1−42) peptides in fibrils suggested from NMR data[50] and the topology of Aβ (1−42) or Aβ (10−35) peptides in small oligomers suggested from simulations using simplified models.[51,52] Strand−loop−strand structures may thus be intermediates for fibril nucleation and elongation.[10] The strand−loop−strand propensity of B18 in aqueous buffer might therefore be an important factor for the ability of this peptide to form amyloid-like fibrils.

Summary

To understand the conformational plasticity of the fibrillogenic−fusogenic Bindin (103−120) B18 peptide, this peptide was studied in different environments using MD simulations. The environments consisted of a water−TFE mixture with an effective TFE concentration between 14 and 30 vol %, pure water, aqueous buffer containing 100 mM NaCl, and a buffer−vapor interface. The peptide was investigated as an isolated molecule in solution or at the interface. The total time scale simulated was about 2 μs. Averaged over all amino acids of the peptide and over time, large portions of the peptide (28−56%) were unstructured. Preformed α-helical conformation was least stable in pure water (11 ± 4%), more stable in the water−TFE mixture (40 ± 2%), and most stable at the buffer−vapor interface (51 ± 13%). The α-helix stabilizing effect of TFE is in qualitative agreement with experiment. In all these environments, α-helical conformation was most stable in the region around residues 113−116, which are mainly hydrophilic.

***β*-Sheet Structures in Water or Buffer.** Extended peptide configurations in water or buffer folded into structures containing β-sheets in agreement with CD data. The β-sheet content was higher in buffer (27 ± 13%) than in water (10 ± 2%) in agreement with data from CD. α−β-Transitions were observed at elevated temperature (350 K). The resulting β-sheet and turn−bend content was similar to that formed from extended configurations at 293 K. Turns were primarily formed by hydrophilic residues (>30% at positions 111−113 in water). In water or buffer, β-sheets were mainly formed by hydrophobic residues (>20% at positions 106−108 and 118−119 in water and >70% at positions 106 and 107 in buffer).

In water, both parallel and antiparallel β-sheets, whereas in buffer only antiparallel β-sheets, formed. Some β-sheets in water or buffer formed twice in identical or similar form, suggesting them to be typical structures in aqueous solution. These structures include antiparallel β-sheets between (i) residues 106−107 and 118−119, (ii) residues 115−119 and 104−108 or 106−111, and (iii) a type II′ β-hairpin formed by residues 104−113. In the β-hairpin, residue R108 in the turn region predominantly formed backbone dihedral angles $\phi = 60 \pm 20°$ and $\psi = -85 \pm 25°$ and thus adopted a conformation partially destabilized by steric interactions of the side chain. Replacing the arginine by a glycine residue (R108G mutant) is expected to stabilize the β-hairpin and thus increase the overall β-sheet content of B18 in buffer. In contrast, no significant change on the β-sheet content is expected for the R111G mutant.

Adsorption to a Buffer−Vapor Interface. When a B18 molecule in a strand−loop−strand conformation was placed in buffer in contact with vapor, it was spontaneously adsorbed to the buffer−vapor interface with the hydrophobic side of the adsorbed peptide pointing toward the interface. The β-sheet content was decreased from (16 ± 4%) in the bulk to (7 ± 4%) at the interface. At the interface, turns formed at positions 108−119. Turn formation preceded α-helix nucleation or a dynamic equilibrium between 3_{10}- and α-helical conformations and single turns in the region around residues 114−117. These observations suggest typical conformational changes during the initial steps of the adsorption. A preformed helix−kink−helix structure of the peptide partially dissolved or converted into a continuous helix. Helix axes were oriented parallel to the interface. The

partial α-helical conformation of the peptide and the in-plane orientation of helix axes are in agreement with results from IRRAS data.[6]

Conclusion

MD simulations of the fibrillogenic fusion peptide B18 indicate that its conformational behavior is strongly dependent on the environment in agreement with experiment and give new structural insights on a microscopic level. α-Helical conformation is induced upon interaction of B18 with trifluorethanol or a buffer−vapor interface and is most preferred by the C-terminal segment, which is hydrophilic. In aqueous solution, B18 has a high tendency to form structures containing β-sheets and turns. Turns are formed by hydrophilic residues; β-sheets are mainly formed by hydrophobic residues. A few typical β-sheets are suggested. Simulations at elevated temperature suggest α−β-conversions of B18 to proceed via a coil intermediate. The propensity of B18 to form β-strand−loop−β-strand structures in aqueous solution might be intimately linked with its ability to form amyloid-like fibrils *in vitro*.

Acknowledgment. The authors thank A. S. Ulrich and S. Afonin for providing the NMR structure of B18 and D. Roccatano for providing the TFE model. Annabel Münter, Gerald Brezesinski, R. Woody, and L. Reich are acknowledged for useful discussions.

References and Notes

(1) Kelly, J. W. *Proc. Natl. Acad. Sci. U.S.A.* **1998**, *95*, 930.
(2) Crescenzi, O.; Tomaselli, S.; Guerrini, R.; Salvadori, S.; D'Ursi, A. M.; Temussi, P. A.; Picone, D. *Eur. J. Biochem.* **2002**, *269*, 5642.
(3) Rocha, S.; Thunemann, A. F.; Pereira, M. C.; Coelho, M. A. N.; Möhwald, H.; Brezesinski, G. *ChemBioChem* **2005**, *6*, 280.
(4) Ulrich, A. S.; Otter, M.; Glabe, C. G.; Hoekstra, D. *J. Biol. Chem.* **1998**, *273*, 16748.
(5) Ulrich, A. S.; Tichelaar, W.; Forster, G.; Zschornig, O.; Weinkauf, S.; Meyer, H. W. *Biophys. J.* **1999**, *77*, 829.
(6) Maltseva, E. Model membrane interactions with ions and peptides at the air/water interface. Ph.D. Thesis, Universität Potsdam, 2005.
(7) Glaser, R. W.; Grune, M.; Wandelt, C.; Ulrich, A. S. *Biochemistry* **1999**, *38*, 2560.
(8) Binder, H.; Arnold, K.; Ulrich, A. S.; Zschornig, O. *Biochim. Biophys. Acta Biomembr.* **2000**, *1468*, 345.
(9) Daidone, I.; Simona, F.; Roccatano, D.; Broglia, R. A.; Tiana, G.; Colombo, G.; Di Nola, A. *Proteins* **2004**, *57*, 198.
(10) Han, W.; Wu, Y. D. *J. Am. Chem. Soc.* **2005**, *127*, 15408.
(11) Xu, Y. C.; Shen, J. J.; Luo, X. M.; Zhu, W. L.; Chen, K. X.; Ma, J. P.; Jiang, H. L. *Proc. Natl. Acad. Sci. U.S.A.* **2005**, *102*, 5403.
(12) Daidone, I.; Amadei, A.; Di Nola, A. *Proteins* **2005**, *59*, 510.
(13) Villa, A.; Mark, A. E.; Saracino, G. A. A.; Cosentino, U.; Pitea, D.; Moro, G.; Salmona, M. *J. Phys. Chem. B* **2006**, *110*, 1423.
(14) Fan, H.; Wang, X.; Zhu, J.; Robillard, G. T.; Mark, A. E. *Proteins* **2006**, *64*, 863.
(15) Kubelka, J.; Hofrichter, J.; Eaton, W. A. *Curr. Opin. Struct. Biol.* **2004**, *14*, 76.
(16) Koradi, R.; Billeter, M.; Wüthrich, K. *J. Mol. Graph.* **1996**, *14*, 51.
(17) Karraker, K. A.; Radke, C. J. *Adv. Colloid Interface Sci.* **2002**, *96*, 231.
(18) Marrink, S. J.; Marcelja, S. *Langmuir* **2001**, *17*, 7929.
(19) Schuler, L. D.; Daura, X.; van Gunsteren, W. F. *J. Comput. Chem.* **2001**, *22*, 1205.
(20) Hermans, J.; Berendsen, H. J. C.; van Gunsteren, W. F.; Postma, J. P. M. *Biopolymers* **1984**, *23*, 1513.
(21) van der Spoel, D.; Lindahl, E.; Hess, B.; Groenhof, G.; Mark, A. E.; Berendsen, H. J. C. *J. Comput. Chem.* **2005**, *26*, 1701.
(22) Hess, B.; Bekker, H.; Berendsen, H. J. C.; Fraaije, J. G. E. M. *J. Comput. Chem.* **1997**, *18*, 1463.
(23) Feenstra, K. A.; Hess, B.; Berendsen, H. J. C. *J. Comput. Chem.* **1999**, *20*, 786.
(24) Feenstra, K. A.; Peter, C.; Scheek, R. M.; van Gunsteren, W. F.; Mark, A. E. *J. Biomol. NMR* **2002**, *23*, 181.
(25) Berendsen, H. J. C.; Postma, J. P. M.; van Gunsteren, W. F.; Nola, A. D.; Haak, J. R. *J. Chem. Phys.* **1984**, *81*, 3684.
(26) Darden, T.; York, D.; Pedersen, L. *J. Chem. Phys.* **1993**, *98*, 10089.
(27) Hünenberger, P. In *Simulation and theory of electrostatic interactions in solution: Computational chemistry, biophysics, and aqueous solutions*; Pratt, L., Hummer, G., Eds.; American Institute of Physics: Santa Fe, NM, 1999; pp 17−83.
(28) Kabsch, W.; Sander, C. *Biopolymers* **1983**, *22*, 2577.
(29) Sreerama, N.; Venyaminov, S. Y.; Woody, R. W. *Protein Sci.* **1999**, *8*, 370.
(30) Woody, R. W. Private communication.
(31) Connolly, M. L. *Science* **1983**, *221*, 709.
(32) Roccatano, D.; Colombo, G.; Fioroni, M.; Mark, A. E. *Proc. Natl. Acad. Sci. U.S.A.* **2002**, *99*, 12179.
(33) Chitra, R.; Smith, P. E. *J. Chem. Phys.* **2001**, *115*, 5521.
(34) *Nachr. Chem. Tech. Lab.* **1997**, *45*, 406.
(35) Armen, R.; Alonso, D. O. V.; Daggett, V. *Protein Sci.* **2003**, *12*, 1145.
(36) Provencher, S. W.; Glockner, J. *Biochemistry* **1981**, *20*, 33.
(37) Sreerama, N.; Woody, R. W. *Anal. Biochem.* **2000**, *287*, 252.
(38) Chou, P. Y.; Fasman, G. D. *Biochemistry* **1974**, *13*, 211.
(39) Barre, P.; Zschornig, O.; Arnold, K.; Huster, D. *Biochemistry* **2003**, *42*, 8377.
(40) Ding, F.; Borreguero, J. M.; Buldyrey, S. V.; Stanley, H. E.; Dokholyan, N. V. *Proteins* **2003**, *53*, 220.
(41) Simona, F.; Tiana, G.; Broglia, R. A.; Colombo, G. *J. Mol. Graph.* **2004**, *23*, 263.
(42) Nguyen, H. D.; Hall, C. K. *Proc. Natl. Acad. Sci. U.S.A.* **2004**, *101*, 16180.
(43) Wu, C.; Lei, H. X.; Duan, Y. *J. Am. Chem. Soc.* **2005**, *127*, 13530.
(44) Monticelli, L.; Tieleman, D. P.; Colombo, G. *J. Phys. Chem. B* **2005**, *109*, 20064.
(45) Flöck, D.; Colacino, S.; Colombo, G.; Di Nola, A. *Proteins* **2006**, *62*, 183.
(46) Wei, G. H.; Shea, J. E. *Biophys. J.* **2006**, *91*, 1638.
(47) D'Ursi, A. M.; Armenante, M. R.; Guerrini, R.; Salvadori, S.; Sorrentino, G.; Picone, D. *J. Med. Chem.* **2004**, *47*, 4231.
(48) Avbelj, F.; Moult, J. *Biochemistry* **1995**, *34*, 755.
(49) Zhang, S.; Iwata, K.; Lachenmann, M. J.; Peng, J. W.; Li, S.; Stimson, E. R.; Lu, Y.; Felix, A. M.; Maggio, J. E.; Lee, J. P. *J. Struct. Biol.* **2000**, *130*, 130.
(50) Luhrs, T.; Ritter, C.; Adrian, M.; Riek-Loher, D.; Bohrmann, B.; Doeli, H.; Schubert, D.; Riek, R. *Proc. Natl. Acad. Sci. U.S.A.* **2005**, *102*, 17342.
(51) Urbanc, B.; Cruz, L.; Yun, S.; Buldyrev, S. V.; Bitan, G.; Teplow, D. B.; Stanley, H. E. *Proc. Natl. Acad. Sci. U.S.A.* **2004**, *101*, 17345.
(52) Jang, S.; Shin, S. *J. Phys. Chem. B* **2006**, *110*, 1955.